doi:10.1093/brain/awx121 BRAIN 2017: 140; 1–3 | e43

BRAIN
A JOURNAL OF NEUROLOGY

LETTER TO THE EDITOR

Capgras syndrome: neuroanatomical assessment of brain MRI findings in an adolescent patient

Mark R. Ferguson,[1] Cassie K. Yu,[2] Andrew V. Poliakov,[1] Seth D. Friedman[1,*] and Jon M. McClellan[3,*]

[*]These authors contributed equally to this work.

1 Department of Radiology, Seattle Children's Hospital, Seattle, USA
2 Department of Psychiatry and Behavioral Health, Seattle Children's Hospital, Seattle, USA
3 Department of Psychiatry, University of Washington, USA

Correspondence to: Mark R. Ferguson, MD
4800 Sand Point Way NE, Seattle, WA 98105
E-mail: markferg@uw.edu

Sir,

We read with great interest the paper by Darby *et al.* (2017). As cases of Capgras delusion are extremely rare, and most literature reports only describe one or two such cases with imaging (Luca *et al.*, 2013; Sottile *et al.*, 2015), this makes the paper of Darby *et al.* (2017) an insightful attempt to use existing data to assemble a larger population of delusional syndrome cases, and use functional connectivity to advance our understanding of the anatomical substrate of this phenomenon. We believe that reporting one such case encountered in our institution could also make a contribution to better understanding of this rare syndrome as lesion location and connectivity pattern do not appear to clearly overlap with reported results.

Materials and methods

The patient is a 16-year-old Somali male with a 1-year history of declining function, social isolation, agitation, lack of self-care and delusional beliefs. He was born and raised in the USA, but had visited Ethiopia in the year prior to his decompensation. He was hospitalized after calling the police to report that his parents were not his real parents. He had no focal neurological findings and a negative laboratory evaluation, including toxicology screen, basic serum chemistries, blood counts, thyroid-stimulating hormone, B12 and folate levels.

The patient was clinically imaged under propofol anaesthesia on a 3 T Siemens TRIO using a 32-channel head coil. The protocol used localizers, axial/coronal transverse relaxation sequences (T_2, 4/1 mm gap, respectively), axial fluid-attenuated inversion images (FLAIR, 4-mm thick), a longitudinal relaxation structural scan (T_1-MP-RAGE, isotropic 1 mm), susceptibility-weighted images (SWI, 2 mm), and a 10-direction diffusion tensor imaging scan (DTI, B = 1000, 3.3 mm). No intravenous contrast was used. Images were reviewed by our study radiologist (M.F.) confirming the original clinical interpretation.

Images were co-registered to standard space using FLIRT algorithm (part of FSL 4.1.4 software package). Affine registration of T_1 MPRAGE image to MNI 152 T_1 template was performed. This transform was utilized for lesion localization in the MNI atlas space, with masking of the entire lesion referenced to the Johns Hopkins white matter atlas. Tracts with majority fractions overlapping the lesion were tabulated. Grey matter cortex neighbouring the white matter lesion was seeded for connectivity exploration using published results (Faria *et al.*, 2012), and the 980 subject connectome atlas (Connectome Workbench v. 1.2.3 software package) (Van Essen *et al.*, 2013).

Results

A $\sim 7 \times 4$ mm focus of T_2/FLAIR hyperintensity is observed within the periventricular white matter along the left lateral ventricle frontal horn (Fig. 1). Corresponding hypointense T_1 signal is present. There is no associated restricted diffusion or signal loss of SWI images. There is no regional or global brain parenchymal atrophy. Finding likely represents gliosis related to a prior non-specific insult.

Advance Access publication June 3, 2017

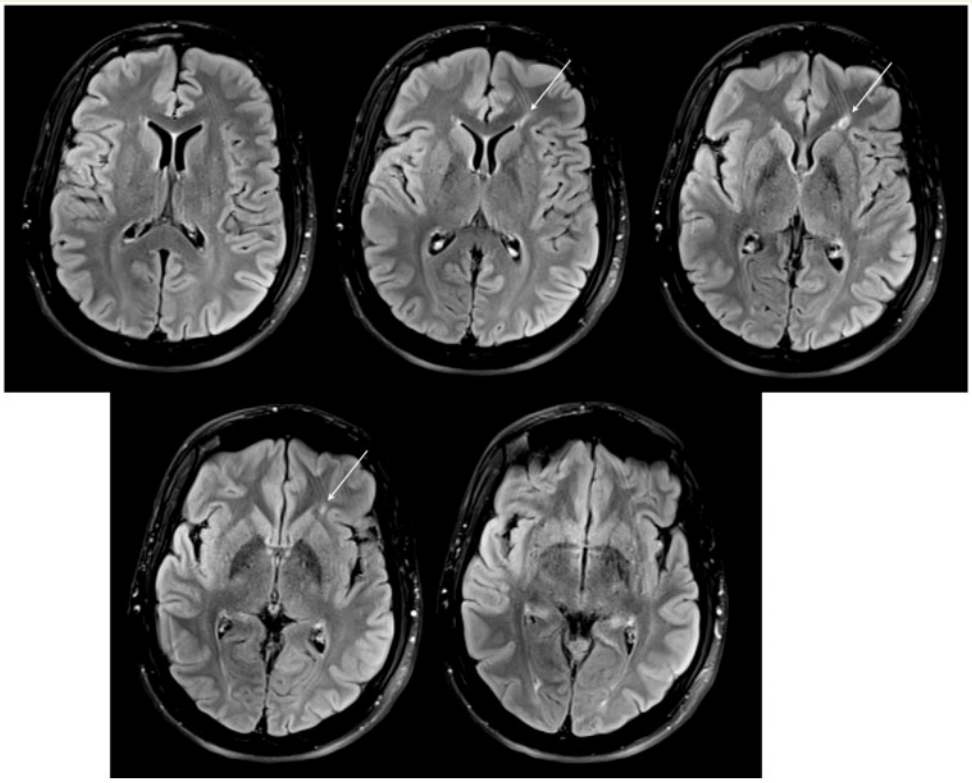

Figure 1 Sequential images showing the lesion (indicated with arrows) present in left frontal white matter.

The location of this lesion in the MNI atlas space was found to be centred at (−22, 32, −3). Seeding the entirety of this lesion using the Johns Hopkins white matter atlas demonstrated that the major tracts coincident with the visible lesion were the inferior fronto-occipital fasciculus (27%) and the uncinate fasciculus (17%) Lesional projection to the grey matter surface implicated Brodmann area 10 (BA10), which includes the middle and inferior frontal gyri. Though we could not readily apply the exact mapping technique of Darby *et al.* (2017), we attempted to infer possible functional connectivity of BA10 using literature data. From published functional connectivity tables (Faria *et al.*, 2012), correlation coefficients were described to the following regions: left middle frontal gyrus → left superior frontal gyrus (correlations coefficient, +0.23), left inferior frontal gyrus (+0.43), left angular gyrus (+0.61), left cuneus (−0.3), left lingual gyrus (−0.3), and right middle frontal gyrus (+0.52). For the left inferior frontal gyrus → left middle frontal gyrus (+0.17), left fronto-orbital gyrus (+0.33), left insula (+0.35), and right inferior frontal gyrus (+0.49). In Connectome Explorer, the high granularity possible in regional selection of BA10 created extensive maps to explore, none of which seemed to strongly implicate right ventral frontal and left retrosplenial connectivity.

Discussion

At the most gross level, the lesion in this teen patient has a different location, extent, and aetiology than the patients presented by Darby *et al.* (2017). Overlaying this lesion location to a white matter tract atlas implicates involvement of the left inferior fronto-occipital fasciculus and uncinate fasciculus tracts. In a recent report, the left inferior fronto-occipital fasciculus tract was identified to be reduced in density in a diffusion tensor analysis of an adult with Capgras delusion but without a visible lesion (Bobes *et al.*, 2016). The uncinate fasciculus connects the anterior temporal lobe with the frontal cortex, and surgical removal of the left uncinate fasciculus is associated with impairments in retrieving the names of famous faces (Papagno *et al.*, 2011). Extrapolating this patient's lesion to grey matter cortex and evaluating normal functional MRI connectivity weights described by Faria *et al.* (2012) or using the Connectome Explorer (Van Essen *et al.*, 2013) demonstrates connectivity to the proximal frontal cortex, mirrored contralateral frontal lobe, and long-range posterior targets, areas that do not clearly overlap with foci identified by Darby *et al.* (2017).

While there are examples in the literature of left-sided causing delusional syndromes (Sottile *et al.*, 2015), the imaging data meeting inclusion criteria for mapping in Darby *et al.* (2017) are mostly right frontal. Given the homogeneity of this sample, adding our additional patient will minimally alter the perceived significance of the results. As the classic structure-function literature often equates the smallest lesion causing a pure behavioural phenotype as gold standard, we hypothesized two main ways to integrate our new data and other existing literature (Sottile *et al.*, 2015; Bobes *et al.*, 2016), leaving open the possibility that both or neither is true: (i)

silent lesions are always present that affect right frontal and left retrosplenial connectivity; or (ii) a separate left-sided route exists that is sufficient in and of itself to create the syndrome. At present, patient-specific resting state functional MRI combined with task-based functional MRI similar to Thiel *et al.* (2014) is probably the only way to partially confirm or deny these suppositions, the challenge being that it is also possible that abnormalities reside substantially below the resolution or sensitivity of functional MRI. As a caveat from the author's previous paper, extensive reorganization of resting networks following brain injury introduces significant challenges for interpreting connectivity variation in the abnormal brain (Boes *et al.*, 2015). For now, such methods provide a novel approach to identify functional regions that may be involved in myriad syndromes. We look forward to continued efforts to synthesize information from disparate patients.

Funding

No funding was received towards this work.

References

Bobes MA, Góngora D, Valdes A, Santos Y, Acosta Y, Fernandez Garcia Y, et al. Testing the connections within face processing circuitry in Capgras delusion with diffusion imaging tractography. Neuroimage Clin 2016; 11: 30–40.

Boes AD, Prasad S, Liu H, Liu Q, Pascual-Leone A, Caviness VS Jr, et al. Network localization of neurological symptoms from focal brain lesions. Brain 2015; 138 (Pt 10): 3061–75.

Darby RR, Laganiere S, Pascual-Leone A, Prasad S, Fox MD. Finding the imposter: brain connectivity of lesions causing delusional misidentifications. Brain 2017; 140 (Pt 2): 497–507.

Faria AV, Joel SE, Zhang Y, Oishi K, van Zjil PC, Miller MI, et al. Atlas-based analysis of resting-state functional connectivity: evaluation for reproducibility and multi-modal anatomy-function correlation studies. Neuroimage 2012; 61: 613–21.

Luca M, Bordone A, Luca A, Patti A, Sortino G, Calandra C. Clinical features and imaging findings in a case of Capgras syndrome. Neuropsychiatr Dis Treat 2013; 9: 1095–9.

Papagno C, Miracapillo C, Casarotti A, Romero Lauro LJ, Castellano A, Falini A, et al. What is the role of the uncinate fasciculus? Surgical removal and proper name retrieval. Brain 2011; 134 (Pt 2): 405–14.

Sottile F, Bonanno L, Finzi G, Ascenti G, Marino S, Bramanti P, et al. Cotard and Capgras syndrome after ischemic stroke. J Stroke Cerebrovasc Dis 2015; 24: e103–4.

Thiel CM, Studte S, Hildebrandt H, Huster R, Weerda R. When a loved one feels unfamiliar: a case study on the neural basis of Capgras delusion. Cortex 2014; 52: 75–85.

Van Essen DC, Smith SM, Barch DM, Behrens TE, Yacoub E, Ugurbil K, et al. The WU-Minn human connectome project: an overview. Neuroimage 2013; 80: 62–79.